



## Structure studies of Pulmonary Surfactant Protein B(SP-B (3,4)) by NMR Spectroscopy and Molecular Modeling

Dongha Baek, Joo Hyun Kang,<sup>1</sup> Song Yub Shin,<sup>2</sup> Kyung-Soo Hahm,<sup>3</sup> Yangmee Kim\*

Department of Chemistry, Konkuk University, Seoul 143-701, Korea

<sup>1</sup>Peptide Engineering Research Unit, Korea Research Institute of Bioscience and Biotechnology,  
KIST, P.O. Box 115, Yusong, Taejon 305-600, Korea

<sup>2</sup>Department of Life Science, KJIST, Kwangju 500-712, Korea

<sup>3</sup>Chosun Bio-materials Research Institute Biotechnology, Kwangju 501-759, Korea

Received March 25, 2001

**Abstract:** Synthetic pulmonary surfactants consisting of a mixture of phospholipids with synthetic peptides based on human surfactant-associated protein SP-B were prepared. These surfactants were analyzed for their secondary structures by circular dichroism (CD) spectroscopy and NMR spectroscopy. Two synthetic peptides (SP-B(3), SP-B(4)) combined with the phospholipid mixture displayed significant surfactant properties. The CD spectra showed that the  $\alpha$ -helical propensities of the peptides in DPC micelles. In the NMR spectroscopy, the tertiary structures of SP-B(3) show that it has  $\alpha$ -helical structure from Gln5 to Arg13 in DPC micelle and SP-B(4) show that they have  $\alpha$ -helical structure from Gln5 to Leu12 in DPC micelle. Based on these structures, truncated peptides originated from SP-B protein, can be designed as effective synthetic surfactants for clinical use.

### INTRODUCTION

Pulmonary surfactant, lowering alveolar surface tension, is essential for prevention of alveolar collapse at the end expiration.<sup>1</sup> A deficiency of surfactant at birth, often due to premature delivery, is responsible for the neonatal respiratory distress syndrome.<sup>2</sup> The pulmonary surfactant is composed of 90-95% phospholipid, mainly dipalmitoyl-phosphatidylcholine(DPPC) and phosphatidylglycerol(PG), and 5-10% protein.<sup>1</sup> The surfactant associated protein is composed of hydrophilic proteins(SP-A and SP-D) and hydrophobic proteins(SP-B and SP-C).<sup>3-9</sup> Synthetic pulmonary surfactant, generally a combination of SP-B, SP-C, and a phospholipid mixture, has been evaluated for their potential use in surfactant replacement therapy.<sup>10</sup> Especially, SP-B resulted in greater surface

\*To whom : ymkim@kkucc.konkuk.ac.kr

tension lowering and better biological activity than SP-C<sup>11</sup>. The truncated peptides (SP-B(3);RMLPQLVCRLVLRCSMD, SP-B(4);RMLPQLVCRLVLRCSM) derived from human SP-B protein, when appropriately recombined with phospholipid, restored the surface tension lowering activity measured by Wilhemly plate method<sup>12</sup>. In order to study the relationship between the structure and biological activity, we performed CD and NMR experiments in TFE solution and DPC micelle. We have determined tertiary structures of SP-B(3,4) using distance geometry and simulated annealing calculation.

## EXPERIMENTALS

### *Peptide synthesis and purification*

Peptides syntheses were performed by the solid phase method using Fmoc as Na-amino protecting group. All the peptides were purified by HPLC on a reverse phase column.

### *CD Experiments*

CD measurements of 0.17mM peptide solutions were performed on a J700 spectropolarimeter(Japan, Jasco) between 190 and 250 nm at 25°C. In order to investigate the conformational changes induced by TFE and DPC(dodecylphosphatidylcholine) micelles, TFE and DPC of the defined composition were added.

### *NMR spectroscopy*

All of the NMR experiments for the sample in 2,2,2-trifluoroethanol-d<sub>3</sub>/H<sub>2</sub>O(1:1 v/v) were performed at 298K and experiments for the samples in DPC micelles were conducted at 308K for SP-B(3) and 298K for SP-B(4). All the phase sensitive two-dimensional experiments such as DQF-COSY, TOCSY and NOESY experiments were performed using time-proportional phase incrementation(TPPI) method.<sup>13-18</sup> For these experiments, 400-512 transients with 2K complex data points were collected for each of the increments with a relaxation delay of 1.2-1.6 sec between the successive transients and the data along the t<sub>1</sub> dimension were zero-filled to 1K before 2D-Fourier transformation. TOCSY experiment was performed using 80-100 msec, MLEV-17 spin-lock mixing pulse. NOESY experiments were performed using a mixing time of 250 msec. The suppression of water signal was achieved by the pulsed field-gradient with WATERGATE sequence for the sample in deuterated DPC micelles.<sup>19</sup> All NMR spectra were recorded on Bruker DPX-400 spectrometer in Konkuk University.

Chemical shifts of the samples were measured relative to the methyl resonance of internal 2,2-dimethyl-2-silapentane-5-sulfonic acid(DSS) at 0 ppm. The <sup>3</sup>J<sub>HN $\alpha$</sub>  coupling constants were either measured in 1D spectrum or calculated by the formula derived by Kim and Prestegard from the separation of absorptive peaks and dispersive peaks in DQF-COSY spec-

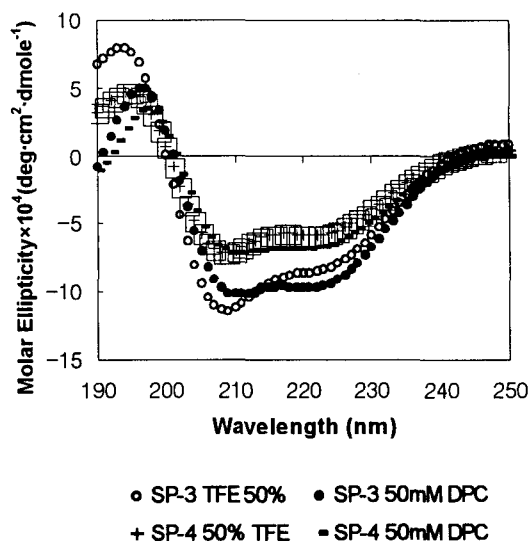


Fig. 1. CD spectra of SP-B(3) and SP-B(4) in 50% TFE and 50mM DPC micelle.

trum.<sup>20</sup> DQF-COSY spectrum was processed to the 4K×2K matrix and used to measure peak-to-peak separations. To identify slowly exchanging amide protons, a series of 1D spectra were acquired after deuterium oxide was added to the sample. All NMR spectra were processed off-line using the FELIX software package (Molecular Simulations Inc., San Diego) on SGI workstation.

#### *Structure calculation.*

Structure calculations were carried out using X-PLOR version 3.851.<sup>21</sup> All the NOE intensities are divided into three classes, i.e., strong, medium, and weak with the distance ranges of 1.8-2.7, 1.8-3.5, and 1.8-5.0 Å, respectively. Standard pseudoatom corrections<sup>22</sup> were applied to the non-stereospecifically assigned restraints, and the additional 0.5 Å was added to the upper bounds for NOEs involving methyl protons. Standard distance geometry-dynamical simulated annealing hybrid protocol<sup>23-26</sup> was employed to generate structures. Center averaging was used to correct distances involving methyl groups and non-stereospecifically assigned methylene. The target function that is minimized during simulated annealing comprises only quadratic harmonic potential terms for covalent geometry, square-well quadratic potentials for the experimental distance and torsion angle restraints, and a quartic van der Waals repulsion term for the non-bonded contacts.

**Table 1.**  $^1\text{H}$  chemical shifts(ppm) for SP-B(3,4) in DPC micelle solution.

Residue	SP-B(3) Chemical shift(ppm) <sup>a</sup> at 308K			
	H	$\alpha\text{H}$	$\beta\text{H}$	Others
Arg <sup>1</sup>		3.96	2.01, 1.92	$\gamma$ * 1.73 $\delta$ * 3.22
Met <sup>2</sup>	9.25	4.46	*2.10	$\gamma$ * 2.60 $\delta$ 0.93, 0.88
Leu <sup>3</sup>	8.68	4.37	*1.77	$\gamma$ * 1.55
Pro <sup>4</sup>		4.27	*2.39	$\gamma$ * 1.92 $\delta$ * 3.70, 3.50
Gln <sup>5</sup>	8.28	3.96	*2.16	$\gamma$ * 2.43
Leu <sup>6</sup>	8.39	4.05	*1.83	$\gamma$ * 1.59 $\delta$ * 0.93, 0.89
Val <sup>7</sup>	7.85	3.56	2.17	$\gamma$ * 1.02, 0.95
Cys <sup>8</sup>	7.96	4.56	3.23, 3.12	
Arg <sup>9</sup>	7.87	4.24	*1.92	$\gamma$ * 1.69 $\delta$ 3.20, 3.14
Leu <sup>10</sup>	7.77	4.37	*1.83	$\gamma$ 1.54 $\delta$ * 0.93, 0.88
Val <sup>11</sup>	7.65	4.36	2.31	$\gamma$ * 0.92, 0.92
Leu <sup>12</sup>	7.92	4.37	*1.78	$\gamma$ 1.61 $\delta$ * 0.93, 0.88
Arg <sup>13</sup>	7.89	4.43	*1.86	$\gamma$ * 1.58 $\delta$ * 3.16
Cys <sup>14</sup>	8.37	4.55	3.42, 3.12	
Ser <sup>15</sup>	8.35	4.43	*3.83	
Met <sup>16</sup>	7.99	4.46	2.09, 1.98	$\gamma$ 2.78, 2.69
Asp <sup>17</sup>	8.31	4.47	2.49, 1.96	

Residue	SP-B(4) Chemical shift(ppm) <sup>a</sup> at 298K			
	NH	$\alpha\text{H}$	$\beta\text{H}$	Others
Arg <sup>1</sup>		4.10	1.93, 2.01	$\gamma$ *1.73 $\delta$ *3.23
Met <sup>2</sup>	9.20	4.49	*2.08	$\gamma$ *2.59
Leu <sup>3</sup>	8.66	4.39	*1.73	$\gamma$ *1.55 $\delta_1$ *0.92 $\delta_2$ *0.92
Pro <sup>4</sup>		4.29	*2.40	$\gamma$ *1.93 $\delta_1$ 3.77 $\delta_2$ 3.53
Gln <sup>5</sup>	8.26	3.99	*2.16	$\gamma$ *2.42
Leu <sup>6</sup>	8.37	4.07	*1.85	$\gamma$ 1.59 $\delta_1$ *0.92 $\delta_2$ *0.89
Val <sup>7</sup>	7.84	3.58	2.18	$\gamma_1$ *1.05 $\gamma_2$ * 0.95
Cys <sup>8</sup>	7.96	4.56	3.20, 3.13	
Arg <sup>9</sup>	7.87	4.26	*1.92	$\gamma$ *1.70 $\delta$ *3.17
Leu <sup>10</sup>	7.77	4.38	*1.78	$\gamma$ 1.54 $\delta_1$ *0.91 $\delta_2$ *0.91
Val <sup>11</sup>	7.65	4.36	2.31	$\gamma_1$ *0.92 $\gamma_2$ *0.92
Leu <sup>12</sup>	7.91	4.37	*1.72	$\gamma$ 1.54 $\delta_1$ *0.89 $\delta_2$ *0.89
Arg <sup>13</sup>	7.89	4.45	*1.89	$\gamma$ *1.59 $\delta$ *3.18
Cys <sup>14</sup>	8.38	4.55	3.41, 3.14	
Ser <sup>15</sup>	8.29	4.46	*3.84	
Met <sup>16</sup>	8.05	4.34	2.09, 1.97	$\gamma$ *2.51

<sup>a</sup>Chemical shifts are relative to DSS(0ppm)

## RESULTS and DISCUSSION

The CD spectra of SP-B(3,4) in 50% TFE solution and 50mM DPC micelle are presented in Fig. 1. SP-B(3,4) has an  $\alpha$ -helical conformation in 50% TFE solution and 50mM DPC micelle. It shows that SP-B(3) has more helicity than SP-B(4).

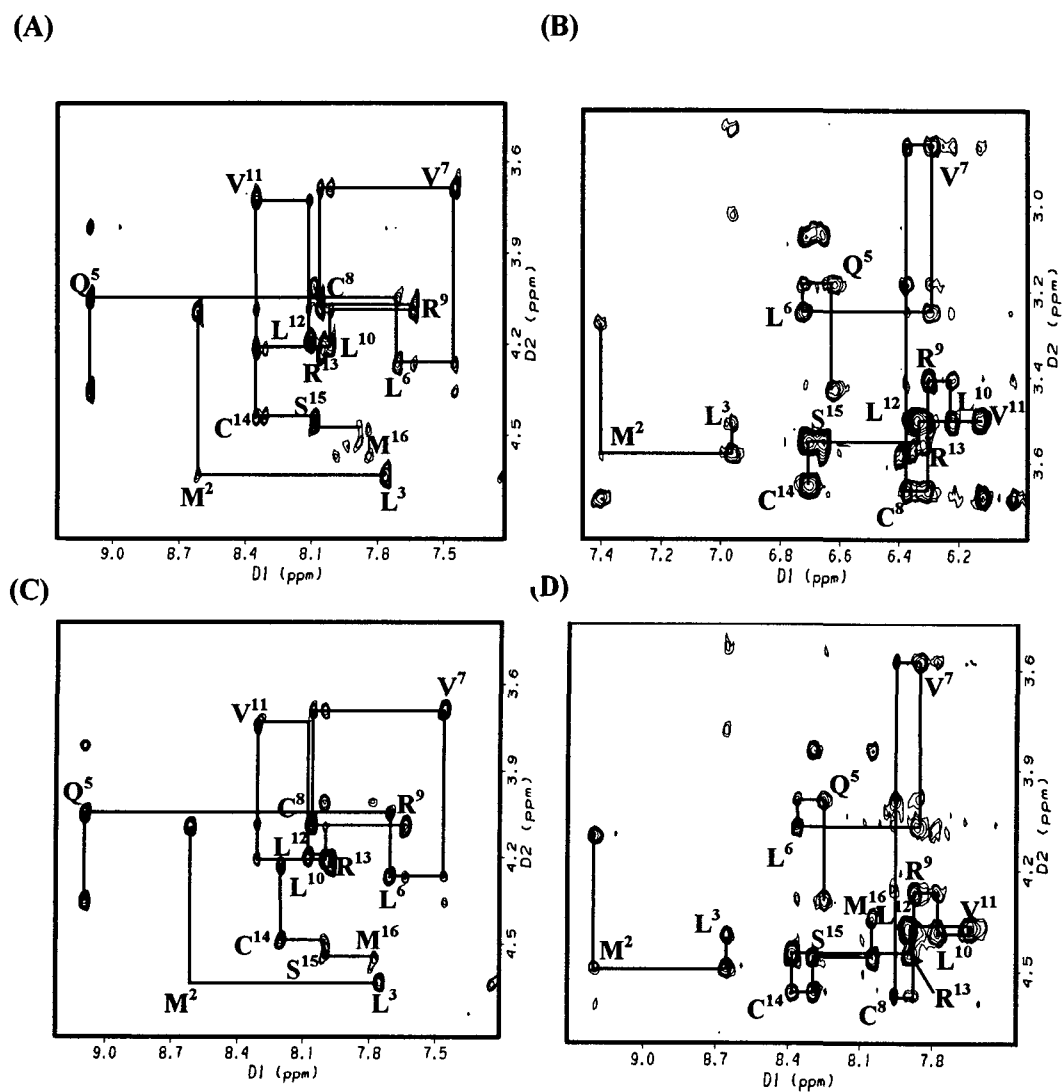
Using standard sequential assignment strategy,<sup>27</sup> all the proton resonances were assigned. TOCSY and DQF-COSY spectra were used to assign spin systems of most of the amino acid residues. By direct comparison of TOCSY and NOESY spectra, sequence-specific resonance assignments were completed. The proton chemical shifts of SP-B(3) at 308K and SP-B(4) at 298K in 90mM DPC micelle are listed in Table 1. The sequential NOE connectivities in the fingerprint region of NOESY spectra of SP-B(3,4) in DPC micelle are illustrated in Fig. 2.

Fig. 3 illustrates the summary of the NOE connectivities of SP-B(3,4) in DPC micelle, which were extracted directly from NOESY spectrum recorded with 250msec mixing time.

A number of nonsequential NOE connectivities characteristic of an  $\alpha$ -helix, i.e., (i,i+3), (i,i+4) correlations, have been observed. The  $d_{\alpha N}(i,i+3)$  connectivities observed from Gln5 to Arg13' in both the SP-B(3) and SP-B(4). Also,  $d_{\beta N}(i,i+3)$  and  $d_{\gamma N}(i,i+3)$  connectivities were found from Leu6 to Leu10. And several  $d_{\alpha N}(i,i+4)$  connectivities observed from Leu5 to Leu12. A dense grouping of  $-1$  values of chemical shifts indices can indicate the presence of  $\alpha$ -helix, and these results agrees with NOE connectivities. Total of 50 structures were generated by hybrid distance geometry-dynamical simulated annealing(SA) algorithm, and 20 structures having lowest energies were selected for further analysis. All 20 SA structures display good covalent geometry and small NMR constraint violations. The mean structure was obtained by restrained minimization of the averaged coordinates of the 20 final structures of each peptide. 20 final structures were fitted over the backbone heavy atoms of Gln5-Leu10 of the mean structures and rmsd from the mean structure of SP-B(3) was 0.19 Å for the backbone atoms(N, C $\alpha$ , C', O) and 1.14 Å for all heavy atoms. In the same region, SP-B(4) showed 0.36 Å for the backbone atoms(N, C $\alpha$ , C', O) and 1.27 Å for all heavy atoms.

The ribbon structure of the restrained minimized mean structures of SP-B(3,4) in DPC micelles are shown in Figure 4. Structures were analyzed using PROCHECK. The tertiary structures of SP-B(3) show that it has  $\alpha$ -helical structure from Gln5 to Arg13 in DPC micelle and the tertiary structures of SP-B(4) show that they have  $\alpha$ -helical structure from Gln5 to Leu12 in DPC micelle.

According to the bioactivity data, SP-B(3) shows much higher surface tension-lowering activity than SP-B(4). Since SP-B(3) has Asp17 in addition compared to SP-B(4), SP-B(3) appears to have a bent structure at the C-terminus. This may cause SP-B(3) to have better surface tension-lowering activity than SP-B(4). Based on these structures, truncated peptides



**Fig. 2.** NH- $\alpha$ H region of 250ms mixing time NOESY spectrum of SP-B(3) in (A) 50% TFE/H<sub>2</sub>O at 298K and (B) DPC micelle at 308K and SP-B(4) in (C) 50% TFE/H<sub>2</sub>O and (D) DPC micelle at 298K.

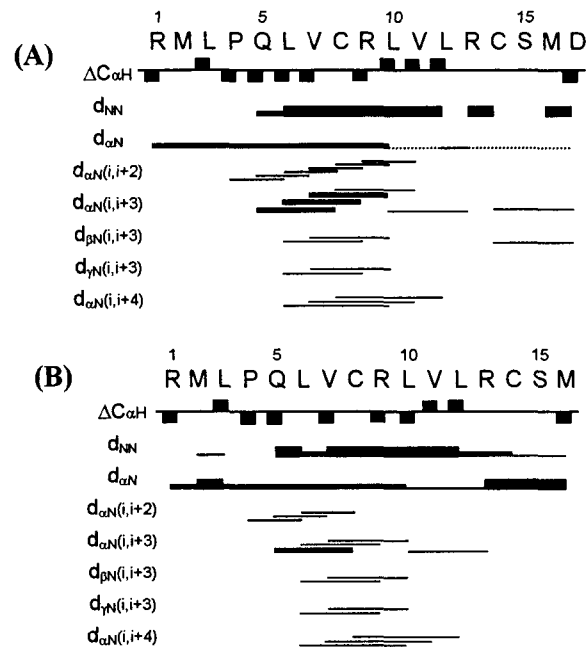


**Fig. 3.** Schematic representation of NOE connectivities of SP-B(3) in (A) 90mM DPC micelle at 308K and SP-B(4) in (B) 90mM DPC micelle at 298K. Line thickness for the NOEs reflects the intensity of the NOE connectivities.

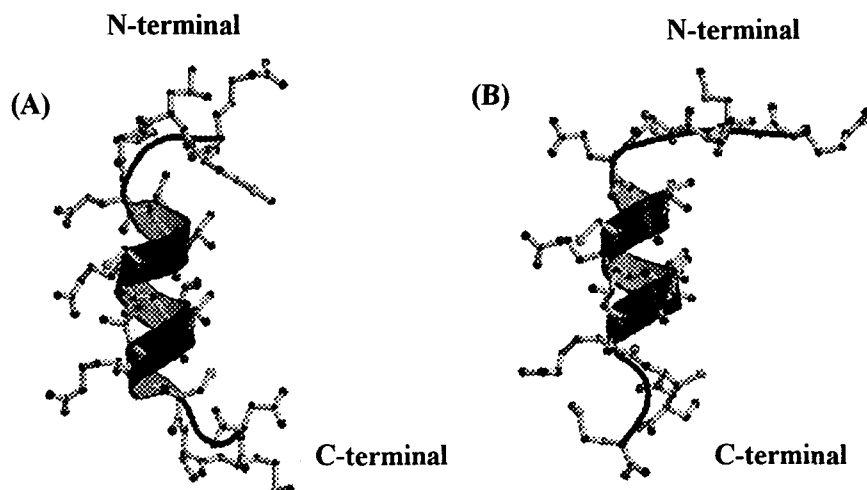


**Fig. 4.** The ribbon structure of the restrained minimized mean structures of (A) SP-B(3) and (B) SP-B(4) in DPC micelles.

originated from SP-B protein, can be designed as effective synthetic surfactants for clinical use.

### *Acknowledgments*

This work was supported by grants from the Ministry of Science and Technology, Korea and the Korea Science and Engineering Foundation through the Research Center for Proteineous Materials.

### REFERENCES

1. Golde, L. M. G., Batenburg, J. J. and Robertson, B. *Physical. Rev.*, **68**, 374-455 (1988).
2. Avery, M. E. and Mead, J. *Am. J. Dis. Child*, **97**, 917 (1959)
3. Phizackerley, P. J. R., Town, M. H. & Newman, G. E. *Biochem. J.* **183**, 731-736 (1979).
4. Suzuki. Y *J. Lipid Res.*, **23**, 62-69 (1982).
5. Tanaka. Y., Takei. T., Aiba. T., Masuda. K., Kuichi. A. & Fujiwara. T. *J. Lipid Res.*, **27**, 475-485 (1986).
6. Takahashi. A & Fujiwara. T. *Biochem. Biophys. Res. Comm.*, **135**, 527-532 (1986).
7. Yu. S-H and Possmayer. F. *Biochem. J.*, **236**, 85-89 (1986).
8. Whitsett. J. A., Ohning. B. L., Ross. G., Menth. J., Weaver. T., Holm. B. A., Shapino D. L. & Notter. R. H. *Pediat. Res.*, **20**, 460-467 (1986).
9. Revak. S. D., Merritt. T. A., Deg ryse. E., Stefani. L., Courtney M., Hallman. M. & Cochrane. C. G. *J. Clin. Incest.*, **81**, 826-833 (1988).
10. Tooley, W. H., Clements, J. A., Muramatsu, K, m Brown, C.L., and Schlueter, M. A. *Amer. Rev. Resp. Dis.*, **136**, 651-656 (1987).
11. Yu, S-H and Possmayer, F. *Biochim. Biophys. Acta.*, **961**, 337-350 (1988).
12. Kang, J. H., Lee, M. K., Kim, K.L., Hahm, K. S. *Biochemistry and molecular biology International*, **40**, 617-627 (1996).
13. A. Derome and M. Williamson, *J. Magn. Reson.*, **88**, 177 (1990).
14. A. Bax and D. G. Davis, *J. Magn. Reson.*, **65**, 355 (1985).
15. S. Macura and R.R. Ernst, *Mol. Phys.*, **41**, 95 (1980).
16. A. Bax and D. G. Davis, *J. Magn. Reson.*, **63**, 207 (1985).
17. G. Bodenhausen and D. J. Ruben, *J. Chem. Phys. Lett.*, **69**, 185 (1980).
18. L. Muller, *J. Magn. Reson.*, **203**, 251 (1987).
19. M. Piotto, V. Saudek, and V. Sklenar, *J. Biomol. NMR*, **2**, 661-666 (1992).
20. Y. Kim and J. H. Prestegard, *J. Magn. Reson.*, **84**, 9 (1989).
21. A. T. Brunger, *X-PLOR Manual, Version 3.1*, Yale University, New Haven, CT, 1993.



22. K. Wüthrich, M. Billeter, W. Braun, *J. Mol. Biol.*, **169**, 949-961 (1983).
23. G. M. Clore and A. M. Gronenborn, *CRC Crit. Rev. Biochem. Mol. Biol.*, **24**, 479 (1989).
24. G. M. Clore and A. M. Gronenborn, *Protein Sci.*, **3**, 372 (1994).
25. G. M. Clore, A. M. Gronenborn, M. Nilges, C. A. Ryan, *Biochemistry*, **26**, 8012 (1987).
26. M. Nilges, G. M. Clore, A. M. Gronenborn, *FEBS Lett.*, **229**, 317 (1988).
27. K. Wuthrich, in "*NMR of Protein and Nucleic acid*", Wiley, New York, 1986.